Detecting quasi-periodic properties of the splitting of separatrices via simultaneous approximation

A. Murillo[1] and A. Vieiro[1]

[1]Departament de Matemàtiques i Informàtica, Universitat de Barcelona (UB), Gran Via, 585, 08007 Barcelona, Spain

May 21, 2026

Abstract

The relation between the linear and the simultaneous approximation of a frequency vector leads to a methodology for detecting changes in the dominant harmonics of the asymptotic behaviour of the exponentially small splitting of invariant manifolds in analytic near-integrable maps F_ε. For a given ε, this reduces to computing the iterate of the map that is closest to the identity near the invariant manifolds. Using this idea, we describe the quasi-periodic properties of the splitting of two-dimensional invariant manifolds of fixed points in concrete families of near-integrable 3D volume-preserving and 4D symplectic maps.

1 Introduction

It is well-known that fast quasi-periodic forcing of integrable analytic Hamiltonian systems with a hyperbolic fixed point leads to an splitting of its separatrices with an exponentially small (in the forcing parameter $\varepsilon \in \mathbb{R}$) upper bound that depends on the frequency vector properties [25, 4]. The splitting behaviour plays an important role in the study of the diffusive properties of the system near the transversal intersection of the invariant manifolds in a near-integrable regime [20]. Moreover, a detailed description of the asymptotic behaviour of the splitting, as $\varepsilon \to 0$, for higher-dimensional invariant manifolds is needed to derive return map models describing the dynamics in the chaotic zone near these invariant manifolds, including the loci of elliptic motions, and explaining how the width of the chaotic zone evolves with the parameter.

The description of the properties of the asymptotic behaviour of the splitting of the invariant manifolds is usually obtained through a detailed analysis of the splitting function and its Poincaré-Melnikov approximation. In concrete applications, one is interested in determining the dominant harmonics in the Fourier series of the splitting function for a given value of the perturbation parameter, which are related to the small divisors associated with the frequencies. If the basic frequencies are rationally independent, the asymptotic behaviour of the splitting is characterized by infinitely many changes of the dominant harmonics of the splitting function, as the perturbation parameter tends to zero [25, 4]. Typically, these changes separate different ε-ranges where the splitting is well-described by a single dominant harmonic (see also comments in Section 3 and prevent the splitting from being governed by a single exponentially small term

(associated with one harmonic). Instead, the envelope of the dominant contributions yields a significantly larger overall splitting exponentially small size.

Direct computations of the exponentially small splitting are cumbersome and hence, as usual, discrete systems appear as a shortcut to avoid the high-precision numerical integration schemes to propagate a flow. However, for a general map, obtaining a detailed description of the splitting function on a fundamental domain is considerably more challenging than in the continuous setting, whether through Melnikov-type approximations or direct numerical computations. A natural alternative is to work with local quantities that quantify the splitting of the invariant manifolds, like computation of suitable angle or areas between (suitable projections of) suitable tangent vectors at the intersection of the invariant manifolds or (generalizations) of the Lazutkin homoclinic invariant [15]. Although these local quantities are sensitive to the quasi-periodic properties of the asymptotic behaviour of separatrix splitting, it is generally unclear how to obtain their analytic expression, and their computation remains expensive.

The purpose of this work is to develop a methodology to detect and characterize the quasi-periodic behaviour of the exponentially small splitting of separatrices in near-integrable families of real-analytic maps F_ε without directly computing it.

Relying only on basic geometrical knowledge of the phase space, the method aims to effectively determine the leading harmonic of the splitting function, which provides an accurate approximation of the splitting function in the ε-ranges where a single harmonic dominates. In particular, it determines whether the asymptotic behaviour of the splitting is expected (under a generic perturbation) to be periodic or quasi-periodic in some limit frequencies.

In this sense, it can be used to study the splitting properties in cases where we do not know the expression of the Melnikov/splitting function (see, for example, Section 6.2) or even when we do not have an explicit expression for F_ε, for example, a Poincaré map obtained by numerical integration.

Moreover, the method detects the presence of harmonics associated with best approximants of the frequency ratio that never become a dominant harmonic of the splitting function, referred to as hidden harmonics [11]. Note that the resonances related to hidden harmonics play a minor role in the dynamics within the chaotic zone around the invariant manifolds. Beyond the amplitude of the splitting, knowing the quasi-periodic properties of the asymptotic behaviour allows one to derive families of adapted higher-dimensional separatrix return maps [27, 3, 1, 2, 24], even in settings where the splitting function cannot be obtained explicitly or is difficult to analyse.

The basic idea of the methodology relies on using the simultaneous approximation of the frequency vector to detect the iterate of the map that becomes closest to the identity. For this purpose, it relies on the relation between the distance to the identity of the map and classical averaging theory [23]. The latter ensures that an analytic family of maps homotopic to the identity can be embedded into a family of autonomous flows, up to an exponentially small error in the distance to the identity parameter. In the ε-ranges where a single harmonic of the splitting function dominates, the autonomous flow is integrable, and the splitting is at most of the order of such an exponentially small approximation error. Therefore, for a near-integrable family of maps F_ε, the smallest error is associated with the iterate that becomes closest to the identity.

In this work, we consider volume-preserving maps in general, which are symplectic whenever the phase space dimension is even. For brevity, we unify both frameworks by referring to them as conservative maps. For concreteness, in this work, we consider families of near-integrable maps related to unfoldings of singularities with complex eigenvalues, although the methodology can

be potentially applied to other systems. Concretely, we use the proposed methodology to reveal the quasi-periodic properties of the asymptotic behaviour of the splitting of separatrices in some 3D volume-preserving and 4D symplectic maps.

The paper is organized as follows. Section 2 describes the properties leading to a quasi-periodic asymptotic behaviour of the splitting of multidimensional invariant manifolds for a one-parameter family of near-integrable maps and presents a methodology, based on the simultaneous approximation of the frequencies involved, to numerically detect such behaviour. Section 3 provides further details on the splitting function and explains how it can be used to obtain the exact quasi-periodic properties using this methodology. Section 4 considers a particular type of discrete systems related to unfoldings of the Hopf-zero and Hamiltonian-Hopf bifurcations. In Section 5, we consider time-T maps of conservative flows and provide a concrete description based on detailed knowledge of the properties of the splitting function for the flow. Finally, more general examples are studied in Section 6 using the proposed methodology.

2 Families of near-integrable maps and simultaneous approximation

Families of integrable maps naturally appear as discretizations of systems obtained by a conservative unfolding of singularities, see Section 4. When the singularity has complex eigenvalues, the unfolding gains rotational symmetries. Denote by $\omega_\theta \in \mathbb{R}^m$ the frequencies of the corresponding angular variables $\theta \in \mathbb{T}^m$ parameterizing the rotational symmetry group. The discretization of the unfolding adds an extra frequency, that we denote as $\omega_\psi \in \mathbb{R}$, that corresponds to the angular variable ψ that defines a suspension of the map. The complete frequency vector is $\Omega = (\omega_\theta, \omega_\psi)$ and, by analogy with the periodically forced flow case that defines the suspension, one considers the splitting function of the invariant manifolds for the discrete system depending on the $(\theta, \psi) \in \mathbb{T}^m \times \mathbb{T}$ variables. The dominant harmonics of the splitting function are related to the linear approximation of Ω. Given a frequency vector $\Omega \in \mathbb{R}^{m+1}$, the linear approximation [17] studies the smallness of scalar products $|k \cdot \Omega|$ for $k \in \mathbb{Z}^{m+1}$, which relates directly to the classical problem of small divisors. The splitting function is said to have a dominant part if there is a finite sum of harmonic terms whose total amplitude is greater than the sum of the amplitudes of all remaining harmonics. If the dominant part consists of one dominant harmonic, it coincides with the leading harmonic, which is the harmonic term of largest amplitude of the splitting function.

Our approach uses the connection between time and phase averaging in dynamics with the interaction between linear and simultaneous Diophantine approximations in number theory. The simultaneous approximation [18] focuses on how well $k\Omega$, with $k \in \mathbb{Z}$, approximates the integer lattice $\mathbb{Z}^{m+1}$ and, in particular, measures how closely the linear flow with frequency Ω returns to its initial position after k iterates. Both perspectives capture the same arithmetic properties of Ω, and are related through transfer principles [17]. Note that an important advantage of simultaneous approximation is that it reduces the detection of near-resonant behaviour in high-dimensional systems to a one-dimensional problem.

In the following, we consider an n-dimensional one-parameter family of real-analytic near-integrable conservative maps F_ε, with $\varepsilon \in \mathbb{R}$. That is, for each ε, there exists $0 < \delta \ll 1$ and an integrable map $F_{\varepsilon,0}$ such that $|F_\varepsilon - F_{\varepsilon,0}| < \delta$. We assume that F_ε has a hyperbolic fixed point for all $\varepsilon > 0$ and that its stable/unstable invariant manifolds, which form an homoclinic/heteroclinic connection in $F_{\varepsilon,0}$, split. Moreover, we assume that, within a compact

domain $\mathcal{D}_\varepsilon \subset \mathbb{R}^n$ around the invariant manifolds depending on ε, the map F_ε can be expressed as a map of $\mathbb{T}^m \times \mathbb{R}^{n-m}$ in terms of angular variables $\theta \in \mathbb{T}^m$.

For a general family of near-integrable maps F_ε of the type considered, the leading harmonic of the splitting function within a range of ε is related to a concrete linear approximation of Ω, hence given by $k \geq 0$ such that $k\Omega \in \mathbb{R}^{m+1}$ approximates a point of the set $\mathbb{Z}^{m+1}$. Then, for such a value of k, F_ε^k becomes a near-the-identity map because its frequency vector is nearly an integer and the action variable remains almost preserved as F_ε is near-integrable. Hence, the method determines the leading harmonic in an ε-range by looking for the positive integer k such that the map F_ε^k is the closest to the identity. In this way, changes in the value of k as $\varepsilon \to 0$ indicate that the splitting of the invariant manifolds is quasi-periodic.

The asymptotic behaviour of the splitting of the invariant manifolds of a family of near-integrable maps F_ε of the type considered will exhibit quasi-periodic properties if:

i) there is a decreasing sequence $\{\varepsilon_j\}_{j\geq 0}$, where ε_0 is small enough and $\lim_{j\to\infty} \varepsilon_j = 0$, such that, for $\varepsilon \in [\varepsilon_{j+1}, \varepsilon_j)$, there exists $q_j = q_j(\varepsilon) \geq 0$ such that $|F_\varepsilon^{q_j} - \mathrm{Id}| \leq |F_\varepsilon^{q} - \mathrm{Id}|$ for all $q \neq q_j$,

ii) the sequence $\{q_j\}_{j\geq 0}$ previously defined is an increasing sequence of integers,

iii) the iterates F_ε^q of the map satisfy that $\lim_{\varepsilon\to 0} |F_\varepsilon^q - \mathrm{Id}| > 0$ for any fixed $q \geq 0$.

The first and second items guarantee that the sequence $q_j(\varepsilon)$ corresponds to a sequence of simultaneous approximations of Ω as $\varepsilon \to 0$. The last condition guarantees that this sequence does not have a limit value q_j, as this would imply a finite number of changes of the leading, and also of the dominant, harmonic.

Remark 2.1. In a different framework, the idea of approximating the dynamics of a map over a domain by covering it with subdomains where a power of the map becomes near-the-identity was recently used in [14] to adapt the proof in [19] of the Nekhoroshev's theorem to the discrete symplectic setting.

However, there is usually a difficulty in directly applying this idea since, in general, the frequencies of F_ε are not explicit. While the frequencies ω_θ can be estimated from the iterates of the map, the other frequency ω_ψ comes from the fact that we are considering a map instead of a flow. As commented, one would like to consider the splitting function depending on the angles (θ, ψ), where ψ is the angular variable implicitly defined through a suspension of F_ε. Typically, there is no direct way to compute the angle ψ. Instead, the methodology we propose defines a suitable observable η, depending on $u \in \mathbb{R}^n$, the coordinates in which F_ε is expressed, that plays the role of a scaled time reflecting the properties of the evolution of ψ. While the specific construction of the observable η depends on the concrete map F_ε, it must satisfy the following geometrical requirements.

We consider an n-dimensional fundamental domain $\Lambda_\varepsilon \subset \mathcal{D}_\varepsilon \subset \mathbb{R}^n$ capturing the dynamics in a region around the invariant manifolds of the fixed point of F_ε. Let $\Sigma \subset \mathbb{R}^n$ be a local transversal section to the $(m+1)$-dimensional invariant manifolds of F_ε. The fundamental domain Λ_ε is given as a tubular domain along the invariant manifolds bounded by the transversal section Σ and $F_\varepsilon(\Sigma)$ and with a small range in the action variables that will be adjusted later. We look for an observable $\eta : \mathbb{R}^n \times \mathbb{R}_+ \to \mathbb{R}$ such that, for all $\varepsilon \leq \varepsilon_0$, there exists a one-to-one correspondence in Λ_ε between the suspension angle ψ and the observable $\eta(u, \varepsilon)$.

The domain of the correspondence can be extended by forward and backward iterations of F_ε. By suitably adjusting the range of the action variables of Λ_ε, we can assume that it is well-defined

for a sufficiently large number of iterates $Q > q_j(\varepsilon)$. This allows us to detect the changes of the leading harmonic of the splitting function by considering an initial point $p \in \Lambda_\varepsilon$ and looking for $q \leq Q$ such that $F_\varepsilon^q(p)$ is the iterate closest to the identity. To this end, we measure the distance of any iterate F_ε^k to the identity through its angular deviation $\Delta F_\varepsilon^k = (\Delta\theta, \Delta\eta)$, since the actions are nearly invariant in the near-integrable regime and their variations are of higher order, so the dominant contribution to the distance to the identity is given by the angular components. For simplicity, we measure this deviation using a weighted ℓ_1-norm,

$$\|\Delta F_\varepsilon^k\|_1 = \sum_{i=1}^{m} \mathrm{w}_i |\Delta\theta_i| + \mathrm{w}_0 |\Delta\eta|,$$

with suitable weights, $\mathrm{w}_i > 0,\ i = 0, \cdots, m$, so that $\Delta\theta_i$ and $\Delta\eta$ are of the same order. Note also that a suitable choice of the initial point is required. In particular, p should be taken sufficiently close to the separatrices so that $p \in \Lambda_\varepsilon$. In practice, we typically select initial points lying on the homo/heteroclinic orbit of a suitable unperturbed system.

In the following sections, we consider concrete examples of near-integrable maps F_ε and, for each of them, we introduce a suitable observable η in a fundamental domain Λ_ε, together with appropriate norm weights. These choices depend on the analytic properties of the splitting function as we discuss in the next section.

3 The ε-values of the changes of leading harmonic.

The asymptotic behaviour of the splitting function for $m = 1$ shows that, if F_ε exhibits quasi-periodic properties, one can consider ε_0 sufficiently small so that there exists a sequence of ε-intervals, with $\varepsilon < \varepsilon_0$, in which the leading harmonic becomes the dominant [25, 4, 5, 6]. Outside these ε-intervals, our method still allows to identify the leading harmonic of the splitting function, although the dominant part is no longer given by a single harmonic. These transition ranges depend on the arithmetic properties of the frequency vector Ω and, in the case of constant type frequency ratio, having a continued fraction expansion with bounded quotients [17], they shrink as $\varepsilon \to 0$. Consequently, the values of ε at which the leading harmonic changes are located close to the regions where the dominant harmonics change. We refer to [12, 22] for concrete examples that will be considered in Section 5. Similar properties are also expected for more than two frequencies, as observed in [7] in a slightly different setting.

As will be explained below, determining the precise values of ε at which the leading harmonic changes requires a thorough understanding of the contribution of each individual harmonic to the total splitting. We show that by comprehensively analyzing the splitting function, we can measure the distance to the identity (in the angular components) in an appropriate way. This is achieved by introducing appropriate weights in the corresponding norm.

Let F_ε be a map of $\mathbb{T}^m \times \mathbb{R}^{n-m}$ as above. We closely follow the ideas in [10], generalized to the higher-dimensional setting, to obtain optimal upper bounds of the splitting that are expected to describe its precise asymptotic behaviour. The parameterization of the invariant manifold W^u of the hyperbolic fixed point provides an embedding $K^u : \mathbb{T}^m \times \mathbb{T} \to \mathbb{T}^m \times \mathbb{R}^{n-m}$ such that

$$F_\varepsilon(K^u(\theta_0, \psi_0)) = K^u(L(\theta_0, \psi_0)),$$

where $L(\theta_0, \psi_0) = (\theta_0 + \omega_\theta, \psi_0 + \omega_\psi)$. Similarly, one obtains a parameterization K^s of W^s. We think of K^u and K^s as periodic functions of the internal angles $\theta_0 \in \mathbb{T}^m$ and an extra angular variable that we denote by $\psi_0 \in \mathbb{T}$.

Assume that both parameterizations can be extended so that they provide graph representations of the invariant manifolds on a common fundamental domain homeomorphic to $\mathbb{T}^m \times \mathbb{T}$, and consider the Fourier expansion of the splitting function

$$\begin{aligned} S(\theta_0, \psi_0) &= K^u(\theta_0, \psi_0) - K^s(\theta_0, \psi_0) \\ &= \sum_{(m_1,m_2)\in\mathbb{Z}^m\times\mathbb{Z}} C_{m_1,m_2} e^{m_1\cdot\theta_0\,\mathrm{i}}\, e^{m_2\psi_0\,\mathrm{i}}\,. \end{aligned}$$

Assume that F_ε is a perturbation of an integrable map $F_{\varepsilon,0}$ that contains an m-dimensional foliation of homo/heteroclinic orbits to the fixed point/s. Since it is integrable, $F_{\varepsilon,0}$ can be exactly interpolated by an autonomous (limit) flow with a m-dimensional foliation of homoclinic orbits $\theta(t) = \omega_\theta t + \theta_0$, $\psi(t) = \omega_\psi t + \psi_0$, in terms of the time variable t of the flow. Then

$$S(\theta_0, \psi_0) \approx \sum_{(m_1,m_2)\in\mathbb{Z}^m\times\mathbb{Z}} C_{m_1,m_2} e^{-(m_1\cdot\omega_\theta + m_2\omega_\psi)\,t\,\mathrm{i}}\, e^{(m_1\cdot\theta + m_2\psi)\,\mathrm{i}}\,.$$

Assuming that the dependence of S on θ, ψ, and t is analytic within the complex strips of width ρ_θ, ρ_ψ, and ρ_t, respectively, a standard application of Cauchy's theorem implies that the amplitude of the (m_1, m_2)-harmonic of the splitting function is bounded as

$$|C_{m_1,m_2}| \le K e^{-|m_1\cdot\rho_\theta| - |m_2|\rho_\psi} e^{-s\rho_t},$$

where $s = |m_1\cdot\omega_\theta + m_2\omega_\psi|$ and K denotes the maximum of $|S|$ in the compact domain inside the path of integration. Assuming that $|C_{m_1,m_2}|$ behaves as the previous upper bound, we see that the leading term of the splitting function is given by the pair $(m_1, m_2) \in \mathbb{Z}^m \times \mathbb{Z}$ that maximizes $|C_{m_1,m_2}|$, or equivalently, minimizes $|m_1 \cdot \rho_\theta| + |m_2|\rho_\psi + s\rho_t$. Since $m_2 = (\pm s - m_1\cdot\omega_\theta)/\omega_\psi$, the leading harmonic of the splitting function corresponds to m_1 and s that minimize

$$|m_1 \cdot (\rho_\theta + \hat{\omega}_\theta\rho_\psi/\omega_\psi)\,| + s\,(\rho_t \pm \rho_\psi/\omega_\psi)\,,$$

where $\hat{\omega}_\theta$ denotes the vector whose components are the absolute value of the components of ω_θ. As explained in Section 2, we aim to detect the leading harmonic by minimizing a suitable weighted ℓ^1-norm. To define appropriate weights, we relate (m_1, s) to the system coordinates (θ, η) so that the contributions of $\Delta\theta$ and $\Delta\eta$ in the norm reflect their influence on (m_1, s). To this end, for each map F_ε, we approximate this dependence by a linear relation of the form $(m_1, s) \approx (A\Delta\theta + b\Delta\eta, a\cdot\Delta\theta + b_0\Delta\eta)$, $A \in \mathbb{R}^{m\times m}$, $a, b \in \mathbb{R}^m$, $b_0 \in \mathbb{R}$, and use the previous expression to define the norm

$$\|\Delta F_\varepsilon^k\|_1 = \mathrm{w}|\Delta\theta| + \mathrm{w}_0|\Delta\eta|, \tag{1}$$

where

$$\begin{aligned} \mathrm{w} &= A\,(\rho_\theta + \hat{\omega}_\theta\rho_\psi/\omega_\psi) + a\,(\rho_t \pm \rho_\psi/\omega_\psi)\,, \quad \text{and} \\ \mathrm{w}_0 &= b\cdot(\rho_\theta + \hat{\omega}_\theta\rho_\psi/\omega_\psi) + b_0\,(\rho_t \pm \rho_\psi/\omega_\psi)\,. \end{aligned}$$

Note that looking for a linear dependence might not be so restrictive since one can always introduce a proper observable η. On the other hand, the weights depend on the analyticity strips, which might be difficult to determine for concrete maps and might require suitable numerical computations. Hence, in a general situation, we only balance the contributions of $\Delta\theta$ and $\Delta\eta$ to the norm to detect the changes of leading harmonic without determining the exact weights. We illustrate the choice of the weights of the norm in examples that are derived as time-T maps of periodically forced vector fields, as in this case, we explicitly know the constants involved.

4 Near-integrable maps from unfoldings of singularities with complex eigenvalues

In this section, we introduce some examples of 3D and 4D near-integrable maps related to unfoldings of singularities with complex eigenvalues with 2D invariant manifolds homoclinic/heteroclinic to one/two fixed point/s. We will investigate the asymptotic behaviour of the exponentially small splitting of their 2D separatrices.

First, we consider two types of examples that can be written explicitly as near-integrable maps. The first type are simply the time-$T = 2\pi/\omega_\psi$ map of a vector field of the form

$$X(u, t, \varepsilon, \delta) = X_0(u, \varepsilon) + \delta X_1(u, \psi(t)),$$

with

$$\psi(t) = \omega_\psi t + \psi_0, \quad \psi_0 \in [0, 2\pi),$$

for small δ fixed and where X_0 is a one-parameter conservative unfolding of a singularity with complex eigenvalues depending on $\varepsilon \in \mathbb{R}$. The properties of the splitting of separatrices of this map can be directly related to the properties of the (Poincaré-Melnikov approach of) the splitting function for the vector field X. A detailed explanation of the methodology applied to examples of this type is given in Section 5.

We consider the Hopf-zero and the Hamiltonian-Hopf singularities as examples of singularities with complex eigenvalues. That is, the vector field X_0 will be a conservative one parameter, ε, unfolding of either the Hopf-zero or the Hamiltonian-Hopf. As said, the splitting of separatrices in these two cases is closely related to the analytical study of the splitting function of the flow X. For the Hopf-zero bifurcation, such a study was carried out in [22]. The study of the splitting of the 2D invariant manifolds created at the Hamiltonian-Hopf bifurcation under a periodic forcing was done in [12].

Since maps arising as time-T maps of periodic flows are non-generic, the second type of family of near-integrable maps considered is derived after performing a discretization of the vector field X_0. This allows us to obtain an explicit map without the additional symmetries of the time-T map but with similar properties to those of the previous one.

Furthermore, we also include two examples of near-integrable maps with fixed point/s with complex eigenvalues that cannot be explicitly written as perturbations of the discretizations considered. The first example is the discretization of the Michelson flow introduced in [21], and the second one is a Froeschlé-like map introduced in [13] but for parameters so that it undergoes a discrete Hamiltonian-Hopf bifurcation. Those examples show the difficulties of projecting the splitting as a function of the angles (θ, ψ) onto a suitable pair (θ, η) of variables, see Section 2.

We detail below the low-order unfoldings of the Hopf-zero bifurcation and the Hamiltonian-Hopf bifurcation that define the vector field X_0 used in the first type of examples and the discretization of the Hopf-zero unfolding used to obtain an example of the second type.

4.1 The unfolding of the Hopf-Zero singularity

The volume-preserving unfolding of the second-order truncated normal form of the codimension-two Hopf-Zero singularity can be written as [16]

$$\begin{aligned} \dot{x} &= y - xz, \\ \dot{y} &= -x - yz, \\ \dot{z} &= -\varepsilon^2 + z^2 + b(x^2 + y^2), \end{aligned} \tag{2}$$

where $\varepsilon \geq 0$. Introducing symplectic polar coordinates in the (x, y)-plane, defined by $(x, y) = (\sqrt{2I}\sin(2\pi\theta), \sqrt{2I}\cos(2\pi\theta))$, it can be written as

$$\dot{\theta} = -1, \quad \dot{I} = -2Iz, \quad \dot{z} = -\varepsilon^2 + z^2 + 2bI. \tag{3}$$

The system possesses a rotational symmetry around the z-axis with frequency -1. It also admits a first integral $H(z, I) = I\left(-\varepsilon^2 + z^2 + bI\right)$, whose constant level sets form a foliation transversal to that generated by the rotational symmetry.

The left plot in Fig. 1 illustrates the main features of the reduced (z, I)-system for $b = 1/2$ and $\varepsilon = 1$. It has two saddle fixed points, $(\pm\varepsilon, 0)$, with two different one-dimensional heteroclinic connections. One of these connections lies on the invariant z-axis, while the other heteroclinic bound a region foliated by periodic orbits and containing an elliptic fixed point $(0, \varepsilon^2)$. Taking into account the action of the rotation group around the z-axis, we can conclude that the periodic orbits observed in the figure are two-dimensional invariant tori of the 3D integrable system (2). On the other hand, the heteroclinic connections not contained in the invariant z-axis correspond to two-dimensional heteroclinic connections to the saddle-focus equilibria of (2). The structure that bounds the 2D heteroclinic connections, along with the foliation by two-dimensional invariant tori inside, is known as a bubble of stability.

To derive an example of the second type, we consider F_0 as a discretization of the previous unfolding of the Hopf-zero singularity at $\varepsilon = 0$. Specifically, we discretize (3) by applying a symplectic Euler integrator with stepsize h to the (I, z)-subsystem, and an explicit Euler step to θ, which yields the volume-preserving map

$$\begin{aligned} \bar{\theta} &= \theta - h \mod 1, \\ \bar{I} &= I/(1 + 2hz), \\ \bar{z} &= z + h\left(-\varepsilon^2 + z^2 + 2b\bar{I}\right). \end{aligned} \tag{4}$$

Moreover, F_0 is a diffeomorphism defined around $I = 0$ provided $|h|$ is small enough. For $\varepsilon = 0$, the origin undergoes a Hopf-one bifurcation, which is the discrete-time analogue of the Hopf-zero bifurcation, characterized by a fixed point with a pair of complex-conjugate eigenvalues of modulus one and a third eigenvalue equal to 1. An unfolding of this bifurcation gives rise to a pair of saddle-focus fixed points, whose two-dimensional invariant manifolds bound a $\mathcal{O}(\varepsilon)$-bubble of stability, with two-dimensional KAM tori organized around a normally elliptic invariant curve.

4.2 The unfolding of the Hamiltonian-Hopf singularity

Consider a 2-dof Hamiltonian system with an equilibria which undergoes a Hamiltonian-Hopf bifurcation. At this bifurcation, the eigenvalues of the linearised Hamiltonian system at the fixed point suffer a Krein collision with negative signature, where a pair of purely imaginary

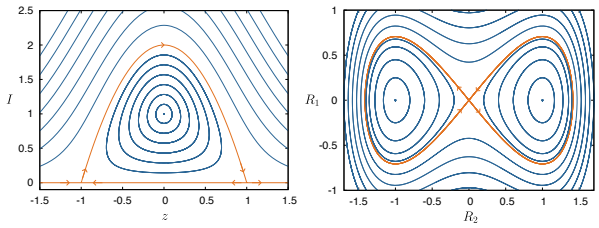

Figure 1: Phase space of the reduced two-dimensional (z, I)-subsystem of system (3) (left) and the Duffing (R_2, R_1)-system (6) (right) for $\varepsilon = 1$, where the homo/heteroclinic orbits between saddle equilibria bound elliptic regions.

eigenvalues meet in a double pair and become a hyperbolic quartet. Then, after the bifurcation, the fixed point becomes a complex unstable hyperbolic point, and it has 2D stable and unstable invariant manifolds.

The normal form reduction of the analysis of the dynamics after the bifurcation leads to the so-called Sokolskii normal form [26, 8]. After the transformation to reduce to such a normal form, the lowest order terms of the unfolding of the Hamiltonian-Hopf bifurcation can be rescaled so that, ignoring $\mathcal{O}(\varepsilon^2)$-terms, are given by the vector field that defines the Hamiltonian [12]

$$H_0 = \Gamma_1 + \varepsilon \left(\Gamma_2 + a\Gamma_3 + \eta\Gamma_3^2\right), \tag{5}$$

with the symplectic form $dx_1 \wedge dy_1 + dx_2 \wedge dy_2$ and where $\Gamma_1 = x_1 y_2 - x_2 y_1$, $\Gamma_2 = (x_1^2 + x_2^2)/2$, $\Gamma_3 = (y_1^2 + y_2^2)/2$ and $\varepsilon > 0$. Notice that for $a < 0$ and $\eta > 0$ the invariant manifolds of the origin are bounded. Introducing

$$\begin{aligned} x_1 &= R_1 \cos(\theta_1), \quad & x_2 &= R_1 \sin(\theta_1), \\ y_1 &= R_2 \cos(\theta_2), \quad & y_2 &= R_2 \sin(\theta_2), \end{aligned}$$

where $R_1,\ R_2 > 0$ and $\theta_1, \theta_2 \in [0, 2\pi)$, one has

$$\begin{aligned} \dot{R}_1 &= \varepsilon R_2(\eta R_2^2 + a)\cos(\theta_2 - \theta_1), \\ \dot{R}_2 &= -\varepsilon R_1 \cos(\theta_2 - \theta_1), \\ \dot{\theta}_1 &= 1 + \varepsilon(\eta R_2^2 + a) R_2 \sin(\theta_2 - \theta_1)/R_1, \\ \dot{\theta}_2 &= 1 + \varepsilon R_1 \sin(\theta_2 - \theta_1)/R_2. \end{aligned}$$

Moreover, the dynamics of the (R_1, R_2)-components restricted to $\{\Gamma_1 = R_1 R_2 \sin(\theta_2 - \theta_1) = 0\}$ is given by the equations associated with the Duffing planar Hamiltonian

$$K = \varepsilon(R_1^2 + aR_2^2 + \eta R_2^4/2)/2. \tag{6}$$

The right plot in Fig. 1 illustrates the main features of the reduced (R_2, R_1)-system for $\varepsilon = 1$, $a = -1, \eta = 1$. The intersection between the two-dimensional invariant manifolds and $\{\Gamma_1 = 0\}$ is given by

$$R_1 = \pm R_2 \sqrt{a + \eta R_2^2/2}.$$

These two-dimensional invariant manifolds separate two-dimensional invariant tori with different topology.

5 The time-T map of a periodically forced flow X

We consider a one-parameter family of analytic near-integrable conservative maps F_ε, with $\varepsilon > 0$, obtained as the time-T stroboscopic map of a periodically forced vector field X. Let

$$X(u, t, \varepsilon, \delta) = X_0(u, \varepsilon) + \delta X_1(u, \psi(t)), \tag{7}$$

with

$$\psi(t) = \omega_\psi\, t + \psi_0, \quad \psi_0 \in [0, 2\pi).$$

where $u \in \mathbb{R}^n$, $\omega_\psi \in \mathbb{R}$, X_0 is an autonomous integrable conservative system, and X_1 is a $2\pi/\omega_\psi$-periodic in time perturbation of the form $X_1(u, \psi) = f(u)g(\psi)$. For concreteness, we assume that for $\delta = 0$ and for each value of ε, the unperturbed system X_0 has a one-dimensional continuum of homo/heteroclinic orbits $\gamma(t, \theta_0, \varepsilon)$ to one/two fixed points, parametrized by an angular variable $\theta_0 \in \mathbb{R}^m$. This surface corresponds to the stable and unstable invariant manifolds of the fixed points, which coincide for the integrable flow X_0. When $\delta \neq 0$, the periodic forcing generically creates a splitting between these invariant manifolds and breaks the homo/heteroclinic connection.

As commented in Section 4, the general form of system (7) is motivated by the analysis of the effect of a periodic forcing of a truncated ε-unfolding of a singularity. Hence, our study considers δ fixed and small, and studies the properties of the splitting for $\varepsilon \to 0$. Let ϕ^t be the flow of $X(u, t, \delta, \varepsilon)$ and define the map

$$F_\varepsilon = \phi^T, \qquad \text{with} \quad T = 2\pi/\omega_\psi,$$

which corresponds to the Poincaré return map to the section $\Sigma_{\psi_0} = \{\psi = \psi_0\}$.

Recall that within the compact domain $\mathcal{D}_\varepsilon \subset \mathbb{R}^n$ around the invariant manifolds, the map F_ε can be expressed as a map of $\mathbb{T}^m \times \mathbb{R}^{n-m}$ and we assume that the dynamics of the angular variables of F_ε tend to the linear dynamics on $\mathbb{T}^{m+1}$

$$\theta \mapsto \theta + \omega_\theta\, T, \qquad \psi \mapsto \psi + \omega_\psi\, T = \psi + 2\pi \equiv \psi,$$

as ε tends to zero. Following the simultaneous approximation approach of Section 2, we look for $k \in \mathbb{Z}$ for which the k-th iterate of the map is close to the identity in the angular variables. This amounts to a simultaneous rational approximation of the frequency vector $\Omega = (\omega_\theta/\omega_\psi, 1)$.

To use the ℓ^1-norm defined in (1), we exploit the specific structure of these maps to compute the norm weights appropriately. The widths of the complex analytic strips ρ_θ and ρ_ψ are determined by the analyticity of the functions $f(u)$ and $g(\psi)$, respectively, while ρ_t corresponds to the singularity of the homo/heteroclinic orbit $\gamma(t, \theta_0, \varepsilon)$. The observable η and its linear dependence on m_1 and s are analysed separately for each map F_ε, as they depend on its geometric properties.

Since the map F_ε is the time-T map of the flow X, the splitting of its two-dimensional invariant manifolds exhibits the same asymptotic exponentially small behaviour as in the flow, including the corresponding changes in the dominant harmonic. In the remaining of this section, we present the results for two cases that have been analysed in detail for the continuous system X, and use this correspondence to understand the differences in the discrete case.

5.1 Periodic forcing of a Hopf-Zero bifurcation

Let X be the three-dimensional vector field with the form

$$X(x, y, z, t, \varepsilon, \delta) = X_0(x, y, z, \varepsilon) + \delta X_1(x, y, z, t),$$

where X_0 is the divergence-free unfolding of the second-order truncated normal form of the Hopf-Zero singularity defined in (2) for $b = 1/2$, and

$$X_1(x, y, z, t) = \left(0,\ 0,\ \frac{y(x^2 + y^2)}{2} f(y)g(\psi)\right)^\top, \tag{8}$$

with $\psi(t) = \omega t + \psi_0$, parameters $\varepsilon, \delta, \omega \in \mathbb{R}$ and an initial time phase $\psi_0 \in [0, 2\pi)$. In particular, we take

$$f(y) = 1/(c - y), \quad \text{and} \quad g(\psi) = 1/(d - \cos(\psi)), \tag{9}$$

with $c > 2\varepsilon$ and $d > 1$ real. Throughout this section we fix $\omega = \sqrt{2}, \delta = 0.01$ and $d = 5$.

The flow X has two saddle-focus fixed points $p_\pm = (0, 0, \pm\varepsilon)$. Since $\mathrm{Spec}(DX(p_\pm)) = \{\pm 2\varepsilon, \mp\varepsilon + \mathrm{i}, \mp\varepsilon - \mathrm{i}\}$, their stable and unstable invariant manifolds satisfy $\dim W^u(p_+) = \dim W^s(p_-) = 1$ and $\dim W^s(p_+) = \dim W^u(p_-) = 2$. In the unperturbed system X_0, the two-dimensional invariant manifolds of p_+ and p_- coincide and form an invariant ellipsoid, which is foliated by the one-parameter family of heteroclinic orbits $\gamma(t, \theta_0, \varepsilon) = (x_\gamma, y_\gamma, z_\gamma)$ with

$$\begin{aligned} x_\gamma &= 2\varepsilon\,\mathrm{sech}(\varepsilon t)\cos(-t + \theta_0), \\ y_\gamma &= 2\varepsilon\,\mathrm{sech}(\varepsilon t)\sin(-t + \theta_0), \\ z_\gamma &= \varepsilon\tanh(\varepsilon t), \end{aligned}$$

where $\theta_0 \in [0, 2\pi)$ is an arbitrary phase. In particular, $\gamma(t, \theta_0, \varepsilon)$ has singularities at $t = (\pi\mathrm{i} + 2\pi k\mathrm{i})/(2\varepsilon), k \in \mathbb{Z}$.

The splitting function of the two-dimensional invariant manifolds of the saddle-foci can be approximated as [22].

$$S(\theta_0, \psi_0, \varepsilon) \approx \delta \sum_{m_1 \geq 0,\, m_2 \in \mathbb{Z}} \hat{C}_{m_1,m_2} G(m_1\theta_0 + m_2\psi_0), \tag{10}$$

where

$$\hat{C}_{m_1,m_2} = (-1)^{\lfloor \frac{m_1+3}{2} \rfloor} \frac{2^5\pi}{\sqrt{d^2-1}(d + \sqrt{d^2-1})^{|m_2|} c^{m_1}} \frac{1}{h(\sigma)} S_P.$$

with $G(\alpha) = \cos(\alpha)$ and $h(\sigma) = \cosh\left(\frac{\sigma\pi}{2\varepsilon}\right)$ if m_1 is odd and $G(\alpha) = \sin(\alpha)$ and $h(\sigma) = \sinh\left(\frac{\sigma\pi}{2\varepsilon}\right)$ otherwise. Moreover,

$$S_P = \sum_{i \geq 0} \frac{(m_1 + 2i)! P_{m_1+2i+4}(\sigma, \varepsilon)}{c^{2i}(m_1 + 2i + 4)!(m_1 + i)!i!}, \quad \sigma = m_2\omega - m_1,$$

where $P_m(\sigma, \varepsilon)$ is recursively defined as

$$\begin{aligned} &P_0 = 1, \qquad P_1 = \sigma, \\ &P_m(\sigma, \varepsilon) = (\sigma^2 + \varepsilon^2(m-2)^2) P_{m-2}(\sigma, \varepsilon), \quad m \geq 2. \end{aligned} \tag{11}$$

The splitting of the two-dimensional invariant manifolds of the saddle-foci is asymptotically exponentially small with quasiperiodic behaviour. As $\varepsilon \to 0$, the dominant harmonic (m_1, m_2) of the splitting function changes due to the balance between the small divisor s and the exponential decay in m_1, m_2. Depending on the arithmetic properties of ω, one can identify an optimal value of $s = |\sigma| = |m_2\omega - m_1|$ that maximizes $|C_{m_1,m_2}|$, giving the leading harmonic of the splitting function for each ε.

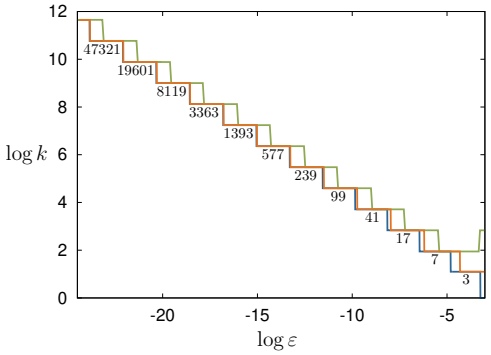

Figure 2: For the time-$2\pi/\omega$ stroboscopic map F_ε of the vector field X with parameters $c = 5\varepsilon$ and $\omega = \sqrt{2}$, we show, as a function of ε, the values of k for which F_ε^k becomes closest to the identity. The distance to the identity is measured using the scaled norm (12) (green) and the weighted norm (14) (orange). For comparison, the blue curve indicates the value of $\log k$ being $k = m_1$ such that (m_1, m_2) is the leading harmonic of the splitting function (10), hence corresponding to a best approximant m_1/m_2 of ω.

Let F_ε denote the time-$2\pi/\omega$ stroboscopic map of the periodically forced vector field X, and we aim to study the quasiperiodic behaviour of the splitting function of the two-dimensional invariant manifolds of F_ε. The vector field X_0 expressed in symplectic polar coordinates, see (3), gives $\omega_\theta = -1$ and $\omega_\psi = \omega$. Then, following the general setting of this Section 5, the frequency vector of the stroboscopic $2\pi/\omega$-map is considered to be $\Omega = (-1/\omega, 1)$. In this setting, the best rational approximants m_1/m_2 of ω are directly related to the small divisors $s/\omega = |-m_1/\omega + m_2| = |(m_1, m_2) \cdot \Omega|$ providing a linear approximation of Ω. These approximants correspond to the dominant harmonics of the splitting function for each ε.

On the other hand, using simultaneous rational approximation, we seek integers k such that $k\Omega = (-k/\omega, k)$ is close to $\mathbb{Z}^2$. If m_1/m_2 is a best approximant of ω, then taking $k = m_1$ yields $k/\omega \approx m_2 \in \mathbb{Z}$ so that $k\Omega \approx (-m_2, m_1) \in \mathbb{Z}^2$. Consequently, when (m_1, m_2) is the dominant harmonic of the splitting function, the iterate $F_\varepsilon^{m_1}$ is the closest to the identity, nearly returning the angular variables to their initial values.

First, we choose as an initial point in the fundamental domain $p_0(\varepsilon) = (2\varepsilon, 2\varepsilon, 0)$, which lies on the heteroclinic orbit γ of the unperturbed system X_0. We then consider

$$\theta = \arctan(y/x) \quad \text{and} \quad \eta(x, y, z) = z,$$

since the z-coordinate along the heteroclinic orbit plays the role of a rotational variable. Note that the range of the variable z, between the two saddle-focus fixed points, is of order $\mathcal{O}(\varepsilon)$, while θ remains of order $\mathcal{O}(1)$. Therefore, we look for $k \in \mathbb{Z}$ that minimizes the weighted norm

$$\|\Delta F_\varepsilon^k\|_1 = |\Delta\theta| + |\Delta\eta|/\varepsilon. \tag{12}$$

For each fixed value of ε, this procedure gives an optimal iterate $k = k(\varepsilon)$ such that F_ε^k behaves as a near-identity map. The corresponding values are shown in green in Fig. 2 for the case $\omega = \sqrt{2}$. The best rational approximants of $\sqrt{2}$ are p_n/q_n, which satisfy the recurrence relations $q_0 = 0$, $q_1 = 1$, $q_n = 2q_{n-1} + q_{n-2}$ with numerators given by $p_n = q_n + q_{n-1}$. We observe that, for sufficiently small ε, the optimal k coincides with m_1, where m_1/m_2 is a best rational approximant of ω. This illustrates the role of simultaneous approximation in detecting the dominant harmonics of the splitting function.

Following Section 3, we compute the weights of the ℓ^1-norm and, relying on the detailed study of the splitting function in [22], we verify that the changes in the leading harmonic identified by our methodology tend to coincide with those of the splitting function as $\varepsilon \to 0$.

First, let us study the width of the analytic strips with respect to θ, ψ, and t. The function $g(\psi)$ is analytic in the complex strip $\{\psi \in \mathbb{C}, \mathrm{Re}(\psi) \in \mathbb{T}, |\mathrm{Im}(\psi)| < \rho_\psi\}$ while the function $f(y)$, with $y = \sqrt{2I}\sin(\theta)$, is analytic in the complex strip $\{\theta \in \mathbb{C}, \mathrm{Re}(\theta) \in \mathbb{T}, |\mathrm{Im}(\theta)| < \rho_\theta\}$, with

$$\rho_\psi = \mathrm{arccosh}(d) \quad \text{and} \quad \rho_\theta = \mathrm{arcsinh}(c/(2\varepsilon)).$$

Note that ρ_θ remains finite when $c = C\varepsilon$ with $C \in \mathbb{Z}$. In Section 5.1.1, we study the case $c \in \mathbb{Z}$, for which f behaves as an entire function. Finally, the width of the analytic strip in the t variable is given by $\rho_t = \pi/(2\varepsilon)$, as it corresponds to the location of the singularities of the heteroclinic orbits γ.

Note that the dynamics of the η-coordinate for the map F_ε can be approximated by $\eta \mapsto \eta - \frac{2\pi}{\omega}\varepsilon^2$ so that after k iterates one has

$$|\Delta\eta| = |\eta(F_\varepsilon^k) - \eta| \approx k\frac{2\pi}{\omega}\varepsilon^2,$$

and

$$|\Delta\theta| = |\theta(F_\varepsilon^k) - \theta| \approx 2\pi|-k/\omega + \tilde{k}|, \qquad \tilde{k} \in \mathbb{Z}.$$

As shown above, the values of k giving the leading harmonic correspond to the integer m_1, so that we obtain the approximations

$$m_1 \approx \omega\,\frac{|\Delta\eta|}{2\pi\varepsilon^2}, \quad s = \omega\,|-m_1/\omega + m_2| \approx \omega\,\frac{|\Delta\theta|}{2\pi}. \tag{13}$$

Thus, the weighted norm introduced in (1) can be written as

$$\|\Delta F_\varepsilon^k\|_1 = \frac{\omega}{2\pi\varepsilon}\left(|\Delta\theta|\mathrm{w} + \frac{|\Delta\eta|}{\varepsilon}\mathrm{w}_0\right). \tag{14}$$

with

$$\mathrm{w} = \pi/2 \pm \varepsilon\,\mathrm{arccosh}(d)/\omega, \quad \text{and}$$
$$\mathrm{w}_0 = \mathrm{arcsinh}(C/2) + \mathrm{arccosh}(d)/\omega.$$

Therefore, as $\varepsilon \to 0$, the above procedure using this weighted ℓ^1-norm allows us to determine a sequence of iterates $k = k(\varepsilon)$ for which F_ε^k is close to the identity. The corresponding values are shown in orange in Fig. 2. We observe that the changes in k tend to coincide with the changes in the leading harmonic of the splitting function, shown in blue as the value of $\log m_1$ associated with the leading harmonic (m_1, m_2) of the splitting function computed in [22], where m_1/m_2 are the best approximants of ω.

5.1.1 Leading harmonic when f tends to an entire function

The splitting function displays different asymptotic behaviours depending on the width of the analyticity strips of the angular variables of the map [6, 25]. In the present example, the function $f(y)$ defined in (9) behaves asymptotically as an entire function as $\varepsilon \to 0$, since the width of its analytic strip is $\rho_\theta = \mathrm{arcsinh}(c/(2\varepsilon))$. Choosing $c \in \mathbb{R}$ constant leads to a logarithmic factor in the numerator of the exponential term of the bound of the splitting function. This suggests using $\Delta\eta|\log\varepsilon|/\varepsilon$ for a better balance comparison with $\Delta\theta$.

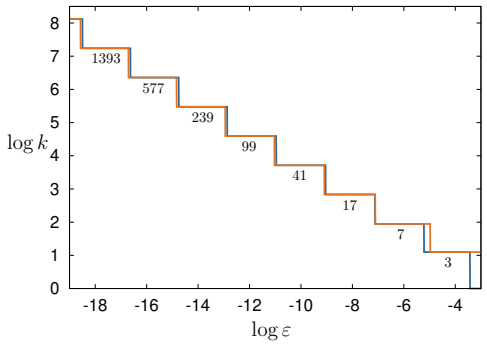

Figure 3: For $c = 0.5$ we display the values of k for which the iterate F_ε^k approximates the identity, plotted as a function of ε. The blue curve represents the value of $\log k$ being $k = m_1$ such that (m_1, m_2) is the leading harmonic of the splitting function (10).

More precisely, if we use the weighted norm defined in (1), together with the same approximations for m_1 and s in terms of $(\Delta\theta, \Delta\eta)$ introduced in (13), we obtain (14) with $C = c/\varepsilon$. Since $\rho_\theta = \operatorname{arcsinh}(c/(2\varepsilon)) \approx |\log\varepsilon| + \log|c|$, the ℓ^1-norm used to determine the iterate closest to the identity can be written as

$$\|\Delta F_\varepsilon^k\|_1 = \frac{\omega}{2\pi\varepsilon}\left(\mathrm{w}|\Delta\theta| + \mathrm{w}_0|\Delta\eta|\right), \tag{15}$$

where the weights are

$$\mathrm{w} = (\pi/2 \pm \varepsilon \operatorname{arccosh}(d)/\omega), \quad \text{and}$$
$$\mathrm{w}_0 = \frac{|\log\varepsilon|}{\varepsilon}(1 + (\log(c) + \operatorname{arccosh}(d)/\omega)/|\log\varepsilon|).$$

The Fig. 3 shows, for $c = 0.5$, the values of k that minimize (15) as a function of ε. For reference, we also display $\log m_1$ in blue, where (m_1, m_2) is the dominant harmonic of the splitting function defined in (10).

Remark 5.1. For a 2π-periodic entire function $f(u) = \sum_{j\in\mathbb{Z}} c_j e^{ju\mathrm{i}}$, the width ρ of its analyticity strip may be chosen depending on j. A standard application of Cauchy's theorem, taking $\rho = \rho(j) \sim \log j$ and using Stirling's approximation, yields the estimate $|c_j| = \mathcal{O}(1/j!)$. In general, any logarithmic growth of the analyticity width ρ with respect to j leads to a factorial decay (with different constants) of the Fourier coefficients of an entire function f.

In our particular example, since $m_1 \sim 1/\sqrt{\varepsilon}$, one has that ρ as a function of ε behaves as $|\log m_1|/2$, and therefore $|c_{m_1}| \sim (m_1!)^{-1/2}$. Then, the amplitude of the (m_1, m_2)-harmonic of the splitting function satisfies

$$|C_{m_1,m_2}| \le K\frac{1}{\sqrt{m_1!}}e^{-|m_2|\rho_\psi}e^{-s\rho_t}.$$

Reasoning as in Section 3, one obtains that the leading harmonic of the splitting function corresponds to values of m_1 and s minimizing

$$\frac{|m_1|}{2}\left(\log|m_1| - 1 + |\omega_\theta|\rho_\psi/\omega_\psi\right) + s\left(\rho_t \pm \rho_\psi/\omega_\psi\right).$$

Therefore, one considers

$$\mathrm{w}_0 = \frac{|\log\varepsilon|}{\varepsilon}(1 + (C_\omega + \operatorname{arccosh}(d)/\omega)/|\log\varepsilon|),$$

with $C_\omega = -1/2 + \log(\omega|\Delta\eta|/(2\pi))/2$, which differs from the weight in the ℓ^1-norm (15) by a term tending to zero as $\varepsilon \to 0$.

5.2 Periodic forcing of a Hamiltonian-Hopf bifurcation

Let X be the $(2+\frac{1}{2})$-degree of freedom Hamiltonian vector field introduced in [12], with Hamiltonian

$$H(x_1, x_2, y_1, y_2, t) = \Gamma_1 + \varepsilon\left(\Gamma_2 - \Gamma_3 + \Gamma_3^2\right) + \delta\, H_1,$$

where

$$H_1 = \frac{y_1^5}{(d - y_1)(c - \cos(\psi))}, \qquad \psi = \omega t + \psi_0,$$

and $H_0 = \Gamma_1 + \varepsilon\left(\Gamma_2 - \Gamma_3 + \Gamma_3^2\right)$ corresponds to the lowest order truncation of the normal form unfolding of a Hamiltonian-Hopf bifurcation (5) with $a = -1$ and $\eta = 1$. Here $\varepsilon > 0$, $\omega \in \mathbb{R} \setminus \mathbb{Q}$, and $\psi_0 \in [0, 2\pi)$ is an initial phase. Throughout this section we fix $\omega = (\sqrt{5}-1)/2, d = 7, c = 5$ and $\delta = 10^{-3}$. Denote by $X_i = J\nabla H_i$, $i = 1, 2$, and $X = J\nabla H$, where J denotes the canonical symplectic matrix. Explicitly, one has a flow $X = X_0 + \delta X_1$ of the form (7) with

$$X_0 = \big(-x_2 + \varepsilon y_1 y_q, x_1 + \varepsilon y_2 y_q, -y_2 - \varepsilon x_1, y_1 - \varepsilon x_2\big)^\top,$$

where $y_q = (y_1^2 + y_2^2 - 1)$ and $X_1 = (f(y_1)g(\psi), 0, 0, 0)$, with

$$f(y_1) = \frac{y_1^4(5d - 4y_1)}{(d - y_1)^2}, \quad g(\psi) = \frac{1}{c - \cos(\psi)}.$$

The 2-dof vector field X_0 admits $F_1 = \Gamma_1$ and $F_2 = \Gamma_2 - \Gamma_3 + \Gamma_3^2$ as independent first integrals around the 2-dimensional invariant manifolds.

The Hamiltonian flow X has a complex saddle fixed point with two-dimensional stable and unstable invariant manifolds. In the unperturbed system, these manifolds coincide and are foliated by the one-parameter family of homoclinic orbits $\gamma(t, \theta_0, \varepsilon) = (x_1(t), x_2(t), y_1(t), y_2(t))$ given by

$$\begin{aligned}
x_1(t) &= -\sqrt{2}\,\mathrm{sech}(\varepsilon t)\tanh(\varepsilon t)\cos(t + \theta_0),\\
x_2(t) &= -\sqrt{2}\,\mathrm{sech}(\varepsilon t)\tanh(\varepsilon t)\sin(t + \theta_0),\\
y_1(t) &= \sqrt{2}\,\mathrm{sech}(\varepsilon t)\cos(t + \theta_0),\\
y_2(t) &= \sqrt{2}\,\mathrm{sech}(\varepsilon t)\sin(t + \theta_0),
\end{aligned}$$

where $\theta_0 \in [0, 2\pi)$ is an arbitrary phase. In particular, $\gamma(t, \theta_0, \varepsilon)$ has singularities at $t = (\pi\mathrm{i} + 2\pi k\mathrm{i})/(2\varepsilon), k \in \mathbb{Z}$. For δ fixed and small, the system was studied in [12], where it was shown that the splitting of the two-dimensional invariant manifolds of the complex saddle fixed point is asymptotically exponentially small with quasiperiodic behaviour. For δ small, the invariant manifolds $W^{u/s}$ can be represented as graphs $g_{u/s} : \mathbb{R}^2 \to \mathbb{R}^2$, $g_{u/s}(\theta_0, \psi_0) = (F_1^{u/s}(\theta_0, \psi_0), F_2^{u/s}(\theta_0, \psi_0))$. Each component of the graph $g_{u/s}$ defines a 2-dimensional surface in $\mathbb{R}^4$. A suitable splitting function $S = (S_1, S_2) : \mathbb{T}^2 \to \mathbb{R}^2$ is defined by

$$S_i(\theta_0, \psi_0) = F_i^u(\theta_0, \psi_0) - F_i^s(\theta_0, \psi_0), \quad i = 1, 2.$$

It was shown in [12] that both components of the splitting function behave asymptotically similar as $\varepsilon \to 0$. Specifically, the leading harmonic of the Taylor-Fourier expansion of S_1 coincides with that of S_2 for large intervals of $\log(\varepsilon)$. Additionally, the difference in the ε-values where each component changes the leading harmonic approaches zero as $\varepsilon \to 0$. More precisely, it was shown that the splitting function S can be approximated as

$$S_i(\theta_0, \psi_0, \varepsilon) \approx \delta \sum_{m_1 \geq 0,\, m_2 \in \mathbb{Z}} \hat{C}^{(i)}_{m_1, m_2} \sin(m_1\theta_0 - m_2\psi_0), \tag{16}$$

where the coefficients $\hat{C}^{(i)}_{m_1,m_2} \in \mathbb{R}$, which depend on ε and $s = |m_2\omega - m_1|$, are related as

$$\hat{C}^{(1)}_{m_1,m_2} = \frac{m_1\varepsilon}{s}\,\hat{C}^{(2)}_{m_1,m_2} + \mathcal{O}(\exp(-\pi s/\varepsilon)).$$

One can see that, for constant type ω, the dominant harmonic has $m_1 \sim 1/s$ and, assuming the dependence of S analytic in a finite complex strip, one has $s \sim \sqrt{\varepsilon}$ and hence both coefficients differ by a constant. Moreover, one has

$$\hat{C}^{(1)}_{m_1,m_2} = \frac{-2\pi\, m_1}{2^{m_1/2}\varepsilon^{m_1}\sqrt{c^2-1}(c+\sqrt{c^2-1})^{|m_2|}d^{m_1-4}}\frac{1}{h(\sigma)}S_P,$$

with $h(\sigma) = \cosh\left(\frac{\sigma\pi}{2\varepsilon}\right)$ if m_1 is odd and $h(\sigma) = \sinh\left(\frac{\sigma\pi}{2\varepsilon}\right)$ otherwise. Moreover,

$$S_P = \sum_{i\geq 0}\frac{(m_1+2i)P_{m_1+2i-1}(\sigma,\varepsilon)}{(2d^2\varepsilon^2)^i(m_1+i)!i!}, \quad \sigma = m_2\omega - m_1,$$

with $P_m(\sigma,\varepsilon)$ as defined in (11).

Let F_ε denote the time-$2\pi/\omega$ stroboscopic map of the periodically forced Hamiltonian H. We aim to study the quasiperiodic behaviour of the splitting function of the two-dimensional invariant manifolds of F_ε. As shown in Section 4.2, for the vector field X_0 written in symplectic polar coordinates and restricted to $\Gamma_1 = 0$, the angular variables satisfy $\theta_1 = \theta_2$ (or $\theta_1 = \theta_2 - \pi$) along the homoclinic orbit. Therefore, in a neighbourhood of the invariant manifolds, we may take the internal angular variable as $\theta = \theta_2$, so that $\omega_\theta = 1$ and $\omega_\psi = \omega$. The frequency vector of the stroboscopic $2\pi/\omega$-map is then $\Omega = (1/\omega, 1)$. In this setting, linear approximations of Ω by the best rational approximants m_1/m_2 of ω are directly related to the small divisors, since $s/\omega = |m_1/\omega - m_2| = |(m_1, -m_2)\cdot\Omega|$.

To use the methodology explained in Section 2, we consider initial points $p_0 = (0, 0, \sqrt{2}, 0)$ lying in the homoclinic orbit γ of the unperturbed system. Then, we introduce the following observable

$$\eta(x_1, x_2, y_1, y_2) = \arctan(R_1/(\sqrt{2} - R_2)),$$

and measure the distance to the identity with the ℓ^1-norm

$$\|\Delta F^k_\varepsilon\|_1 = |\Delta\theta| + |\Delta\eta|. \tag{17}$$

For a given ε, the procedure gives an optimal value $k = k(\varepsilon)$ such that F^k_ε is the closest iterate to the identity. As illustrated by the green curve in Fig. 4, we observe that, for sufficiently small ε, this iterate coincides with m_1, where m_1/m_2 denotes a best approximant of $\omega = (\sqrt{5}-1)/2$. The approximants of the golden frequency are the ratio of consecutive Fibonacci numbers.

Moreover, to compute the weights of the above norm, we follow the approach of Section 3. First, note that the evolution of the η-coordinate can be approximated by

$$\eta \mapsto \eta + \frac{2\pi}{\omega}\left(\frac{R_2(1-R_2^2)(R_2-\sqrt{2}) - R_1^2}{(R_2-\sqrt{2})^2 + R_1^2}\right)\varepsilon.$$

Taking into account the relation between R_1 and R_2 along the separatrix determined by the Duffing Hamiltonian (6), and assuming $R_2 \approx \sqrt{2}$, it follows that after k iterates $\Delta\eta \approx k\varepsilon\frac{\pi}{\omega}$.

On the other hand, the function $g(\psi)$ is analytic in the complex strip $\{\psi \in \mathbb{C}, \mathrm{Re}(\psi) \in \mathbb{T}, |\mathrm{Im}(\psi)| < \rho_\psi\}$ while the function $f(y_1)$, with $y_1 = R_2\cos(\theta)$, is analytic in the complex strip $\{\theta \in \mathbb{C}, \mathrm{Re}(\theta) \in \mathbb{T}, |\mathrm{Im}(\theta)| < \rho_\theta\}$, with

$$\rho_\psi = \mathrm{arccosh}(c) \quad \text{and} \quad \rho_\theta = \mathrm{arccosh}(d/\sqrt{2}).$$

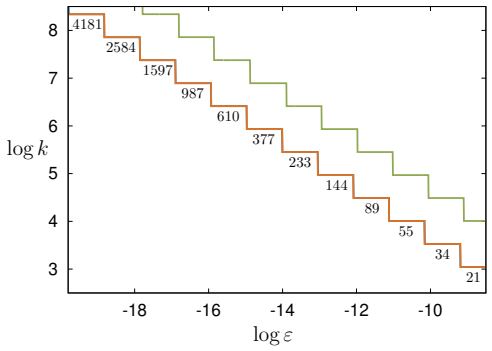

Figure 4: For the time-$2\pi/\omega$ stroboscopic map F_ε of the Hamiltonian H with $\omega = (\sqrt{5}-1)/2$, we show, as a function of ε, the values of k for which F_ε^k is closest to the identity. This distance is measured using the norm (17) (green) and the weighted norm (18) (orange). Within the range of ε displayed, the changes detected using the weighted norm visually coincide with the ones of the splitting function (16) (displayed in blue behind the orange ones).

Finally, the width of the analytic strip in the t variable is given by the location of the closest singularity to the real axis of the homoclinic orbits γ, which is $\rho_t = \pi/(2\varepsilon)$.

Hence, using the approximations $m_1 \approx \omega\frac{\Delta\eta}{\pi\varepsilon}$ and $s \approx \omega\frac{\Delta\theta}{2\pi}$, the weighted norm introduced in (1) can be written as

$$\|\Delta F_\varepsilon^k\|_1 = \frac{\omega}{2\pi\varepsilon}\left(|\Delta\theta|\mathrm{w} + |\Delta\eta|\mathrm{w}_0\right). \tag{18}$$

with

$$\begin{aligned}\mathrm{w} &= \pi/2 \pm \varepsilon\,\mathrm{arccosh}(c)/\omega, \quad \text{and}\\ \mathrm{w}_0 &= 2(\mathrm{arccosh}(d/\sqrt{2}) + \mathrm{arccosh}(c)/\omega).\end{aligned}$$

This weighted ℓ^1-norm provides the sequence of iterates $k = k(\varepsilon)$ displayed in orange in Fig. 4, for which the map F_ε^k is close to the identity and, as $\varepsilon \to 0$, the values at which k changes tend to align with changes in the dominant harmonic of the splitting function (16).

6 Examples of general discrete maps

6.1 A map with a Hopf-one bifurcation

Consider a three-dimensional volume-preserving map F_ε defined as a perturbation of the discretization of the unfolding of the Hopf-zero singularity introduced in (4) for $b = 1/2$. Concretely, $F_\varepsilon : (x, y, z) \mapsto (\bar{x}, \bar{y}, \bar{z})$ is given by

$$\begin{aligned}\bar{x} &= \frac{x\cos(h) + y\sin(h)}{\sqrt{1+2hz}},\\ \bar{y} &= \frac{-x\sin(h) + y\cos(h)}{\sqrt{1+2hz}},\\ \bar{z} &= z + h\left(-\varepsilon^2 + z^2 + \frac{x^2+y^2}{2(1+2hz)} + \delta\frac{\bar{y}(\bar{x}^2+\bar{y}^2)}{2(c-\bar{y})}\right).\end{aligned}$$

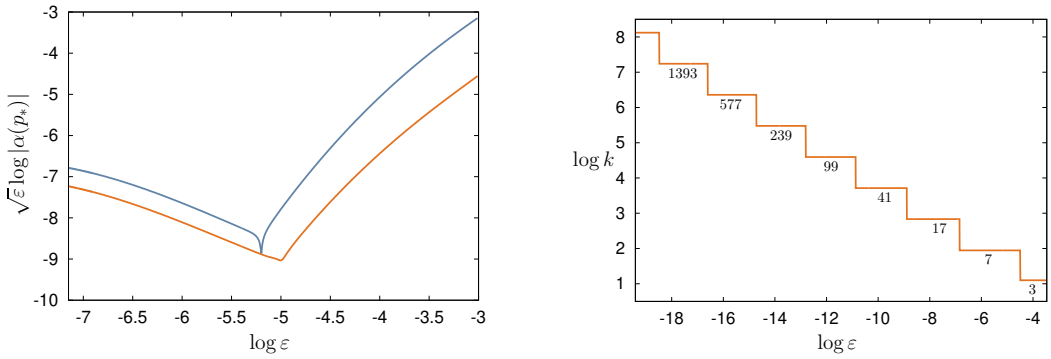

Figure 5: In the left plot we show the Σ-area $\mathcal{A}(p_*)$ in orange and the splitting angle $\alpha(p_*)$ in blue for an heteroclinic orbit p_* of the map F_ε with parameters $h = 2\pi/\omega, \delta = 0.1, c = 0.5$ and $\omega = \sqrt{2}$. In the right plot, we display the values of k for which the iterate F^k approximates the identity, as a function of ε for $\omega = \sqrt{2}$.

The perturbation corresponds to a discretization of the autonomous vector field perturbation δX_1 defined in (8), with $g(\psi) = 1$. Consequently, F_ε provides an approximation of the time-h map of the vector field X studied in Section 5.1, suggesting that the map has a similar geometry and splitting behaviour. Throughout this section we fix $\delta = 0.1$, $d = 5$, $c = 0.5$ and $h = 2\pi/\omega$, with $\omega = \sqrt{2}$. The map F_ε has two saddle-focus fixed points $(x, y, z) = (0, 0, \pm\varepsilon)$, each with a one-dimensional and a two-dimensional invariant manifold sharing the same geometric structure as in the flow, see Fig. 1.

To study the splitting between the two-dimensional invariant manifolds one can compute a suitable local quantity at a homo/heteroclinic orbit. Following [22], we compute the splitting Σ-area $\mathcal{A}(p_*)$ and the splitting angle $\alpha(p_*)$ at a heteroclinic orbit p_*. Let us recall that the splitting Σ-area is defined as the signed area of the parallelepiped that form the normalized tangent vectors to the curves $W^u(p_-) \cap \{z = 0, \psi = \psi_*\}$ and $W^s(p_+) \cap \{z = 0, \psi = \psi_*\}$ at p_* and the splitting angle is the angle between the corresponding tangent planes at p_*. The results are shown in the left plot of Fig. 5. The results suggest a quasi-periodic behaviour of the splitting with the first change in the leading harmonic close to $\varepsilon = \exp(-5)$, but computations for smaller values of ε require much more precision and computing time.

We use the methodology introduced to further investigate the quasi-periodic properties of such splitting. Taking

$$\theta = \arctan(y/x), \quad \text{and} \quad \eta(x, y, z) = z,$$

one has $\omega_\theta = -h/(2\pi)$. The dynamics of the (θ, η)-coordinates can be approximated by the linear dynamics

$$\eta \mapsto -h\varepsilon^2, \quad \theta \mapsto -h \mod 2\pi,$$

so that after k iterates one has

$$|\Delta\eta| \approx kh\varepsilon^2, \quad |\Delta\theta| \approx 2\pi|-hk/(2\pi) + \tilde{k}| = 2\pi s, \quad \tilde{k} \in \mathbb{Z}.$$

Moreover, one checks that $\rho_t = \pi/(2\varepsilon)$ and $\rho_\theta = \operatorname{arcsinh}(c/(2\varepsilon)) \approx |\log\varepsilon| + \log(c)$. Therefore, we are in the regime where f behaves as an entire function, as described in Section 5.1.1, and the appropriate scaling of $\Delta\eta$ is $\Delta\eta|\log\varepsilon|/\varepsilon$. Finally, since ψ is an angular variable defined implicitly through a suspension of F_ε, we consider $\rho_\psi = 0$ in the ℓ^1-norm introduced in (1). Then, we define

$$\|\Delta F_\varepsilon^k\|_1 = \frac{1}{h\varepsilon}\left(|\Delta\theta|\frac{\pi}{2} + \frac{|\Delta\eta|}{\varepsilon}(|\log\varepsilon| + \log(c))\right).$$

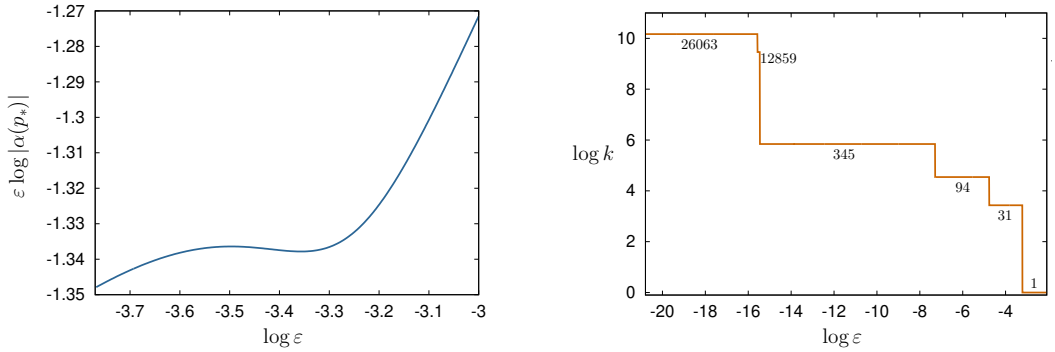

Figure 6: In the left plot, we show the Σ-area $\mathcal{A}(p_*)$ for a heteroclinic orbit p_* of the Michelson map F_ε with $h = 0.2$. In the center plot, we display the values of k for which the iterate F^k approximates the identity as a function of ε with $h = 0.2$ fixed.

The results obtained using this norm are shown in the right plot of Fig. 5. We observe that, for $h = 2\pi/\omega$, the splitting between the two-dimensional invariant manifolds is quasi-periodic, and the dominant harmonics are determined by the best rational approximants of the frequency $\omega = \sqrt{2}$.

6.2 The Michelson map

We consider the Michelson map $F_\varepsilon : (x, y, z) \mapsto (\bar{x}, \bar{y}, \bar{z})$ given by

$$\begin{aligned} \overline{x} &= x + hy, \\ \overline{y} &= y + h\bar{z}, \\ \overline{z} &= z + h(\varepsilon(1 - x^2) - y). \end{aligned}$$

which depends on parameters $\varepsilon \geq 0$ and h. For $\varepsilon > 0$ and $h > 0$ small, the map F_ε has two saddle-focus fixed points $p_\pm = (\pm 1, 0, 0)$, each with a one-dimensional and a two-dimensional invariant manifolds. This map was introduced in [21], and it is obtained as a volume-preserving discretization, with stepsize h, of the divergence-free Michelson vector field

$$X_M(x, y, z, \varepsilon) = (y, z, \varepsilon(1 - x^2) - y).$$

It is well-known that X_M has a perturbed bubble of stability, see for example [9], bounded by the two-dimensional invariant manifolds of the saddle-focus fixed points. Note also that, for $\varepsilon = 0$, the phase space is foliated by invariant planes $x + z = c$, $c \in \mathbb{R}$, where the (y, z)-subsystem reduces to a harmonic oscillator. For h small, the global phase space structure of F_ε resembles that of the Michelson flow.

As in the previous section 6.1, to study the splitting between the two-dimensional invariant manifolds of F_ε, one can compute the splitting Σ-area $\mathcal{A}(p_*)$ at a heteroclinic orbit p_*. Following [9], we consider $\Sigma = \{(x, y, z) \in \mathbb{R}^3 : g(x, y, z) = 0\}$ with

$$g(x, y, z) = x + (1 - 2\varepsilon^2)z - \varepsilon(y + \varepsilon)(2x + 3z/2), \tag{19}$$

because, for ε and h small, the first intersection of the invariant manifolds with Σ are closed curves that are homotopic to a circle. The results, shown in the left plot of Fig. 6, suggest a quasi-periodic behaviour of the splitting function with the first change in the leading harmonic

close to $\varepsilon = \exp(-3.35)$, but computations for smaller values of ε require much more precision and computing time. Hence, we use the methodology explained in this work.

First, we consider the internal angle

$$\theta = \arctan(z/y),$$

which tends to the angular variable of the harmonic oscillator as $\varepsilon \to 0$. Because of the geometrical analogy with the example 6.1, we consider the observable

$$\eta(x, y, z) = g(x, y, z),$$

where g is defined in (19), since it gives the distance to the section Σ. The transversality of Σ for small values of h guarantees a well-defined projection onto the η direction of the splitting along the ψ variable associated with the suspension of the map. On the other hand, introducing the coordinates $(s, \theta, r) = (x+z, \arctan(z/y), \sqrt{y^2+z^2})$ in the Michelson system and neglecting the terms of order $\mathcal{O}(\varepsilon/r)$, the reduced system admits the first integral $H(s, r) = r^2(1 - s^2 - r^2/4)$. Accordingly, we choose the initial point $p_0 = (0, 2, 0)$ on the separatrix of the reduced (s, r) subsystem.

Then, we measure the distance to the identity of the iterates of the point p_0 with the norm

$$\|\Delta F_\varepsilon^k\|_1 = |\Delta\theta| + |\Delta\eta|.$$

The right plot of Fig. 6 shows a sequence of integers k so that F_ε^k is the closest iterate of the map to the identity for a given value of ε.

To understand the relation of k with the frequency vector $\Omega = (\omega_\theta, 1)$, we consider ω_θ^0 to be the limit frequency of ω_θ as $\varepsilon \to 0$. Concretely, one has $\omega_\theta^0 = \log\mu/(2\pi\mathrm{i})$ where μ is the complex eigenvalue with positive imaginary part of the origin for $F_{\varepsilon=0}$. Hence, the values of k giving the closest iterate to the identity correspond to m_2 such that m_1/m_2 are best approximations of ω_θ^0.

For $h = 0.2$ one has $\omega_\theta^0 \approx 0.03188428$ and its first approximants are

$$\frac{1}{31}, \frac{2}{63}, \frac{3}{94}, \frac{11}{345}, \frac{410}{12859}, \frac{831}{26063}, \frac{37805}{1185694}, \dots$$

We observe that all the previous approximants except the second one are detected in Fig. 6. As expected, the best approximant prior to one with m_2 relatively large becomes dominant for a large range of ε. Indeed, simulations up to $\log(\epsilon) \approx -48$ show no changes of k, indicating that the harmonic corresponding to 831/26063 is the dominant one in a large range of $\log(\varepsilon) < -16$.

6.3 A Froeschlé-like map with a Hamiltonian-Hopf bifurcation

As a final example, we consider the four-dimensional symplectic map $F_\varepsilon : (\psi_1, \psi_2, J_1, J_2) \mapsto (\bar\psi_1, \bar\psi_2, \bar J_1, \bar J_2)$ given by

$$\begin{aligned} \bar\psi_1 &= \psi_1 + \delta(\bar J_1 + a_2 \bar J_2), \quad & \bar\psi_2 &= \psi_2 + \delta(a_2 \bar J_1 + a_3 \bar J_2), \\ \bar J_1 &= J_1 - \delta\sin(\psi_1), & \bar J_2 &= J_2 + \delta\,(4/9 + \varepsilon)\sin(\psi_2), \end{aligned}$$

with $a_2 = 1/2$, $a_3 = -3/4$ and $\delta = 1/2$. The map F_ε admits the reversibility $R(\psi_1, \psi_2, J_1, J_2) = (-\psi_1, -\psi_2, J_1 - \delta\sin(\psi_1), J_2 + \delta(4/9 + \varepsilon)\sin(\psi_2))$, that leaves fixed all the points of the plane

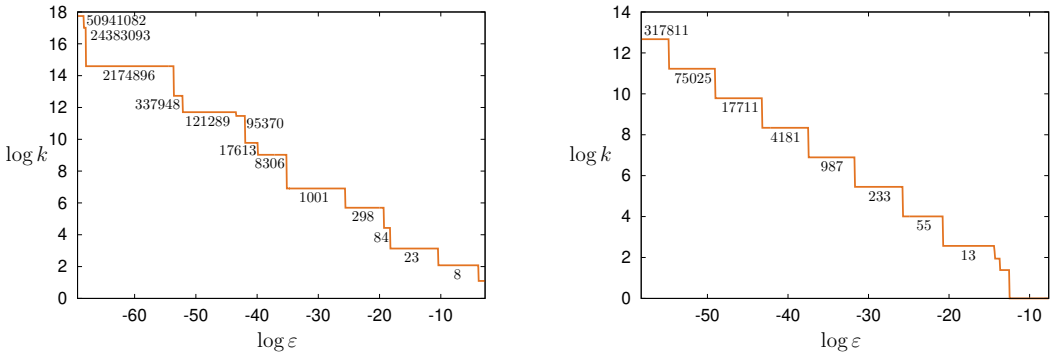

Figure 7: For the Froeschlé-like map F_ε, we display, as a function of ε, the values of k for which the iterate F_ε^k becomes the closest to the identity. In the left plot $\delta = 0.5$, such that $\omega_\theta^0 = \arctan(\sqrt{23}/11)/\pi$ and in the right plot we use $\delta \approx 2.02166$ such that $\omega_\theta^0 = (\sqrt{5}-1)/2$. The values of k correspond to the best approximants of the limit frequency ratio.

$\Pi_R = \{\psi_1 = \psi_2 = 0\}$. At $\varepsilon = 0$ the fixed point at the origin undergoes a discrete Hamiltonian-Hopf bifurcation: for $\varepsilon < 0$ the origin is elliptic, for $\varepsilon = 0$ there is a Krein collision with negative signature at the angle $\beta = \arctan(\sqrt{23}/11)$ of the eigenvalues at the origin, and for $\varepsilon > 0$ the origin becomes a complex-saddle fixed point, with two-dimensional stable and unstable invariant manifolds.

The map F_ε was obtained as a first-order truncated model for the dynamics of a 4D symplectic map at the intersection of two resonances of different but similar orders [13]. Concretely, it corresponds to a symplectic Euler discretization, with stepsize δ, of the Hamiltonian flow generated by

$$H(\psi_1, \psi_2, J_1, J_2) = \frac{J_1^2}{2} + a_2 J_1 J_2 + a_3 \frac{J_2^2}{2} - \cos(\psi_1) - \epsilon \cos(\psi_2).$$

The parameters considered are such that $a_3 - a_2^2 < 0$ (non-definite quadratic part in actions), and it can be shown that there are $\epsilon_c^{(2)} < \epsilon_c^{(1)} < 0$ such that, for $\epsilon \in (\epsilon_c^{(2)}, \epsilon_c^{(1)})$, the fixed point at the origin is of complex-saddle type. For the values of a_2 and a_3 considered one has $\epsilon_c^{(1)} = -4/9$, which justifies that we study the map F_ε above for small values of $\varepsilon = \epsilon_c - \epsilon > 0$. The linear change of coordinates [12]

$$\begin{aligned} x_1 &= \frac{1}{2}\,\psi_1 - \frac{1}{3}\,\psi_2, \quad & x_2 &= -\frac{1}{\sqrt{6}}\,J_1 - \frac{\sqrt{3}}{2\sqrt{2}}\,J_2, \\ y_1 &= \frac{5}{4}\,J_1 - \frac{9}{8}\,J_2, \quad & y_2 &= \frac{3\sqrt{3}}{4\sqrt{2}}\,\psi_1 + \frac{5}{2\sqrt{6}}\,\psi_2, \end{aligned} \tag{20}$$

reduces the quadratic part of H to $H_2 = -\sqrt{2/3}\Gamma_1 + \Gamma_2$. Hence, a near-identity change of coordinates and the rescaling $x_i \mapsto \varepsilon x_i$, $y_i \mapsto \sqrt{3\varepsilon/2}\, y_i$ leads to an unfolding of the Hamiltonian-Hopf bifurcation defined by the Hamiltonian H_0 in (5) with $a = -9/32$ and $\eta = 5/1024$.

Our goal is to investigate the quasiperiodic behaviour of the splitting function associated with the two-dimensional invariant manifolds of F_ε. The previous relation of F_ε and the Hamiltonian (5) allows us to understand the geometry of the map. In particular, we choose below the initial condition $p_0(\varepsilon) = (0, 0, 6\sqrt{6\varepsilon/5}, -12\sqrt{2\varepsilon/15})$, which is located at the intersection between the separatrix of the Duffing part of the unperturbed Hamiltonian H_0 and the section Π_R. On the other hand, because the Hamiltonian-Hopf geometry and following Section 5.2, we introduce the internal angular variable

$$\theta = \arctan(y_2/y_1),$$

and consider

$$\eta(x_1, x_2, y_1, y_2) = (x_1 y_1 + x_2 y_2)/R_2,$$

where $R_2 = \sqrt{y_1^2 + y_2^2}$. Note that the range of the variable η is related to the size of the Duffing loop, which is of order $\mathcal{O}(\varepsilon)$, while θ remains of order $\mathcal{O}(1)$. Then, we measure the distance to the identity of the iterates of the map with the weighted norm introduced in (1),

$$\|\Delta F_\varepsilon^k\|_1 = |\Delta\theta| + |\Delta\eta|/\varepsilon.$$

Let (u_1, u_2, v_1, v_2) be coordinates such that the linear dynamics of $F_{\varepsilon=0}$ is reduced to a Jordan normal form. In the plane $\Pi_u = \{u_1 = u_2 = 0\}$, the linear dynamics in these coordinates is a rotation with frequency $\omega_\theta^0 = \beta/\pi$. We can measure such an angular frequency by looking at the frequency of the projected motion onto any non-orthogonal transversal plane through the origin. We used the angular variable θ in the plane $\Pi_x = \{x_1 = x_2 = 0\}$, expressed in the coordinates (20) as the linear dynamics of H in this plane is a rotation. For δ relatively small, the motion on Π_u projects onto Π_x, then the frequency ω_θ of the angular variable θ we have introduced in Π_x tends to ω_θ^0 as $\varepsilon \to 0$. As for a map $\omega_\psi = 1$, one has $\Omega = (\omega_\theta, 1)$. Accordingly, in the left plot of Fig. 7 we observe values of k that are denominators of approximants of ω_θ^0. The first best approximants of $\omega_\theta^0 = \arctan(\sqrt{23}/11)/\pi \approx 0.130869$ are

$$\frac{1}{7}, \frac{1}{8}, \boxed{\frac{2}{15}}, \frac{3}{23}, \frac{11}{84}, \boxed{\frac{14}{107}}, \frac{39}{298}, \frac{131}{1001}, \frac{1087}{8306},$$

$$\frac{2305}{17613}, \boxed{\frac{3392}{25919}}, \frac{12481}{95370}, \frac{15873}{121289}, \frac{44227}{337948}, ..$$

where we have indicated the approximants not detected, which we conjecture correspond to hidden harmonics [11] of the splitting function, namely harmonics associated with best approximants of the frequency that, despite being expected to dominate, never do so for any value of ε.

The results for $\omega_\theta = (\sqrt{5} - 1)/2$, which is the limit frequency for $\delta \approx 2.0216638371$, are shown in the right plot of Fig. 7. The results indicate that after a detected harmonic, there are two consecutive hidden ones. We believe that the fact that there are hidden harmonics even for the golden frequency is related to the symmetries of the Froeschlé-like map F_ε considered.

Despite the presence of hidden harmonics in both cases, one observes a regular pattern for constant type frequencies as in the right plot. In contrast, an irregular pattern is seen in the left plot, alternating short and longer steps in a quasi-random way.

7 Conclusions

In this paper, we have shown how the simultaneous approximation of a given frequency vector is related with the distance to the identity of a family of integrable maps. We have used this relation to determine the dominant harmonic of the splitting of multi-dimensional invariant manifolds of a fixed point of a discrete map that admits a m-dimensional rotational symmetry group. Moreover, we have described the relations between the discrete splitting function for a conservative map and the splitting function for a periodically forced divergence-free flow, and used this relation to translate the quasi-periodic asymptotic properties of the splitting.

Finally, we have illustrated the methodology in a collection of different examples, and discuss the difficulties that appear in each case.

The simple simulations performed for each example allow us to detect some of the quasi-periodic properties of the asymptotic behaviour of the splitting of the two-dimensional invariant manifolds. In particular, the methodology helps to detect hidden harmonics of the splitting functions, that is, harmonics that never become leading.

The methodology presented, maybe combined with a posteriori numerical fitting of the amplitude of the splitting, can serve as a basic tool to obtain an approximate description of the exponentially small asymptotic behaviour in more involved systems. We emphasize that such an approximation is usually enough to describe the dynamics within the chaotic zone around the invariant manifolds using adapted return separatrix maps [27, 3, 24]. In these regions, the dynamics is highly non-ergodic due to stickiness around the small resonant structures (generalizations of islands of stability to higher dimensions), leading to anomalous diffusion properties, which might depend on the quasi-periodic properties of the splitting behaviour and to possible generalizations of the well-known power-like tails of Poincaré recurrences in the planar area-preserving case, a topic in which Prof. V. Afraimovich made relevant contributions [1, 2].

The ideas discussed in this paper were motivated by the numerical difficulties to investigate the splitting of multidimensional invariant manifolds in some concrete examples, mainly, in studying the splitting of the invariant manifolds of the saddle-focus fixed points created at a volume-preserving Hopf-zero bifurcation and the splitting of the invariant manifolds of the complex-unstable point created at a Hamiltonian-Hopf bifurcation. We believe that similar ideas can be applied in other contexts, for example, to numerically investigate the splitting of homoclinic orbits to invariant tori in Hamiltonian systems, both in discrete and continuous settings.

Acknowledgements

A.M. and A.V. are supported by the Spanish grant PID2021-125535NB-I00 funded by MICIU/AEI/10.13039/501100011033 and by ERDF/EU. A.M. grant is also funded by "ESF+".

References

[1] V. Afraimovich and G. M. Zaslavsky. Fractal and multifractal properties of exit times and Poincaré recurrences. *Phys. Rev. E (3)*, 55(5):5418–5426, 1997.

[2] V. Afraimovich and G. M. Zaslavsky. Space-time complexity in Hamiltonian dynamics. *Chaos*, 13(2):519–532, 2003.

[3] B.V. Chirikov. A universal instability of many-dimensional oscillator system. *Phys. Rep.*, 52:264 – 379, 1979.

[4] A. Delshams, V. Gelfreich, À. Jorba, and T.M. Seara. Exponentially small splitting of separatrices under fast quasiperiodic forcing. *Communications in Mathematical Physics*, 189:35–71, 10 1997.

[5] A. Delshams and P. Gutiérrez. Exponentially small splitting for whiskered tori in Hamiltonian systems: continuation of transverse homoclinic orbits. *Discrete Contin. Dyn. Syst.*, 11(4):757–783, 2004.

[6] A. Delshams and P. Gutiérrez. Exponentially Small Splitting of Separatrices for Whiskered Tori in Hamiltonian Systems. *Journal of Mathematical Sciences*, 128(2):2726 –2745, 2005.

[7] Amadeu Delshams, Marina Gonchenko, and Pere Gutiérrez. Exponentially small splitting of separatrices associated to 3D whiskered tori with cubic frequencies. *Comm. Math. Phys.*, 378(3):1931–1976, 2020.

[8] J.C. Van der Meer. *The Hamiltonian Hopf Bifurcation.* Lecture Notes in Mathematics, 1160. Springer-Verlag, 1985.

[9] F. Dumortier, S. Ibáñez, H. Kokubu, and C. Simó. About the unfolding of a Hopf-zero singularity. *Discrete Contin. Dyn. Syst.*, 33(10):4435–4471, 2013.

[10] E. Fontich and C. Simó. The splitting of separatrices for analytic diffeomorphisms. *Ergodic Theory Dynam. Systems*, 10(2):295–318, 1990.

[11] E. Fontich, C. Simó, and A. Vieiro. On the "hidden" harmonics associated to best approximants due to quasi-periodicity in splitting phenomena. *Regul. Chaotic Dyn.*, 23(6):638–653, 2018.

[12] E. Fontich, C. Simó, and A. Vieiro. Splitting of the separatrices after a Hamiltonian-Hopf bifurcation under periodic forcing. *Nonlinearity*, 32(4):1440–1493, 2019.

[13] V. Gelfreich, C. Simó, and A. Vieiro. Dynamics of 4D symplectic maps near a double resonance. *Physica D*, 243(1):92–110, 2013.

[14] V. Gelfreich and A. Vieiro. Nekhoroshev theory and discrete averaging. *Discrete Contin. Dyn. Syst.*, 2025. To appear.

[15] V. G. Gelfreich, V. F. Lazutkin, and M. B. Tabanov. Exponentially small splittings in Hamiltonian systems. *Chaos*, 1(2):137–142, 1991.

[16] J. Guckenheimer. On a codimension two bifurcation. In *Dynamical systems and turbulence, Warwick 1980 (Coventry, 1979/1980)*, volume 898 of *Lecture Notes in Math.*, pages 99–142. Springer, Berlin-New York, 1981.

[17] A.Y. Khinchin. *Continued Fractions.* The University of Chicago Press, Chicago, Ill.-London, 1964.

[18] P. Lochak. Canonical perturbation theory via simultaneous approximation. *Russian Mathematical Surveys*, 47(6):57, dec 1992.

[19] P. Lochak and A.I. Neishtadt. Estimates of stability time for nearly integrable systems with a quasiconvex hamiltonian. *CHAOS*, 2:495, 1992.

[20] Pierre Lochak. Effective speed of Arnol d's diffusion and small denominators. *Phys. Lett. A*, 143(1-2):39–42, 1990.

[21] J.D. Meiss, N. Miguel, C. Simó, and A. Vieiro. Accelerator modes and anomalous diffusion in 3D volume-preserving maps. *Nonlinearity*, 31(12):5615–5642, 2018.

[22] A. Murillo and A. Vieiro. Periodic perturbation of a 3D conservative flow with a heteroclinic connection to saddle-foci. *Commun. Nonlinear Sci. Numer. Simul.*, 143:Paper No. 108620, 26, 2025.

[23] A.I. Neĭshtadt. The separation of motions in systems with rapidly rotating phase. *J. Appl. Math. Mech.*, 48(2):133–139, 1984.

[24] G.N. Piftankin and D.V. Treschev. Separatrix maps in Hamiltonian systems. *Russian Math. Surveys IOP*, 2(62):219–322, 2007.

[25] C. Simó. Averaging under fast quasiperiodic forcing. *Hamiltonian Mechanics: Integrability and Chaotic Behavior*, Springer US:13–34, 1994.

[26] A.G. Sokolskiĭ. On the stability of an autonomous Hamiltonian system with two degrees of freedom in the case of equal frequencies. *J. Appl. Math. Mech.*, 38:741–749, 1974. Translated from Prikl. Mat. Meh. 38, 791–799 (Russian), 1974.

[27] G. M. Zaslavskiĭ and N. N. Filonenko. Stochastic Instability of Trapped Particles and Conditions of Applicability of the Quasi-linear Approximation. *Soviet Journal of Experimental and Theoretical Physics*, 27:851, 1968.